RADAR IMAGING FOR COMBATTING TERRORISM

Hugh D. Griffiths[†] and Chris J. Baker
Department of Electronic and Electrical Engineering
University College London, London, UK

Abstract. Radar, and in particular imaging radar, have many and varied applications to counterterrorism. Radar is a day/night all-weather sensor, and imaging radars carried by aircraft or satellites are routinely able to achieve high-resolution images of target scenes, and to detect and classify stationary and moving targets at operational ranges. Short-range radar techniques may be used to identify small targets, even buried in the ground or hidden behind building walls. Different frequency bands may be used, for example high frequencies (X-band) may be used to support high bandwidths to give high range resolution, while low frequencies (HF or VHF) are used for foliage penetration to detect targets hidden in forests, or for ground penetration to detect buried targets.

The purpose of this contribution is to review the fundamental principles of radar imaging, and to consider the contributions that radar imaging can make in four specific aspects of counterterrorism: through-wall radar imaging, radar detection of buried targets, tomography and detection of concealed weapons, and passive bistatic radar.

Key words: radar imaging, ground penetrating radar, passive bistatic radar

1. Introduction

Radar techniques and technology have been developed over many decades. Radar has the key attributes of day/night, all-weather performance, and also the ability to measure target range accurately and precisely. The techniques of imaging radar date back to the Second World War, when crude radar images were obtained on the displays of airborne radar systems, allowing features such as coastlines to be distinguished. A major advance took place in the 1950s, when Wiley in the USA made the first experiments with airborne synthetic aperture radar (Wiley, 1985), and nowadays synthetic aperture radar is an important part of the radar art, with radar imagery from satellites and from aircraft routinely used for geophysical remote sensing and for military surveillance purposes. The enormous advances that have been made in imaging radar since the 1950s owe a great deal to the development of fast, high-performance digital processing hardware and algorithms.

[†] Shortly to take up an appointment as Principal of the Defence College of Management and Technology, Shrivenham, Cranfield University, UK.

The objective of this chapter is to review the application of imaging radar systems to counterterrorism. In so doing, we need to bear in mind the things that radar is good at doing, and the things that it is not good at doing. At a fundamental level, then, we will be concerned with the electromagnetic properties of the targets of interest, and of their contrast with the surroundings. We will be concerned with how these properties vary with frequency, since targets may exhibit resonances (and hence enhanced signatures) at certain frequencies, and with the propagation characteristics through materials such as building walls and soil. Hence, we will be interested in techniques which allow us to distinguish targets from the background, by exploiting differences in signature, and wherever possible making use of prior knowledge. It is likely that additional information may be obtained from multiple perspective views of targets (Baker et al., 2006). Further information may be obtainable through the use of techniques such as radar polarimetry and interferometry.

There are two distinct stages to this: (i) the production of high-quality, artefact-free imagery, and (ii) the extraction of information from imagery. It should not be expected that radar images should look like photographs. Firstly radar frequencies are very different from those in the optical region. Secondly, radar is a coherent imaging device (just like a laser) and therefore exhibits multiplicative speckle noise (just like a laser). This makes for an extremely challenging image interpretation environment.

The structure of the chapter is therefore as follows. Firstly, we provide a brief review of the fundamentals of radar imaging, establishing some of the fundamental relations for the resolution of an imaging radar system. This is followed by a discussion of four specific applications to counterterrorism: (i) the detection of buried targets; (ii) through-wall radar imaging; (iii) radar tomography and the detection of concealed weapons; (iv) passive mm-wave imaging; and (v) passive bistatic radar. This is followed by some discussion and some comments on future prospects.

2. Fundamentals of radar imaging

Firstly we can establish some of the fundamental relations for the resolution of an imaging radar system. In the down-range dimension, resolution Δr is related to the signal bandwidth B, thus

$$\Delta r = \frac{c}{2B} \tag{1}$$

where c is the velocity of propagation. High range resolution may be obtained either with a short-duration pulse or by a coded wide-bandwidth signal, such as a linear FM chirp or a step-frequency sequence, with the appropriate pulse compression processing. A short-duration pulse requires a high peak transmit power and instantaneously-broadband operation; these requirements can be relaxed in the case of pulse compression. With the advances in digital processing power it is now relatively straightforward to generate wideband coded waveforms and to perform the pulse compression processing in the receiver in real time.

In the first instance cross-range resolution is determined by the product of the range r and the beamwidth θ_B (in radians). The beamwidth is determined by the dimension d of the antenna aperture and thus the cross-range resolution is given by

$$\Delta x = r\theta_B \approx \frac{r\lambda}{d} \tag{2}$$

where λ is the wavelength. As the dimensions of most antennas are limited by practical considerations (such as fitting to an aircraft) the cross range resolution is invariably much poorer than that in the down range dimension. However, there are a number of techniques that can improve upon this. All of these are ultimately a function of the change in viewing or aspect angle.

The cross range resolution achieved in synthetic aperture radars is determined by the relative motion between the radar and the object. Consider the scenario in Figure 1.

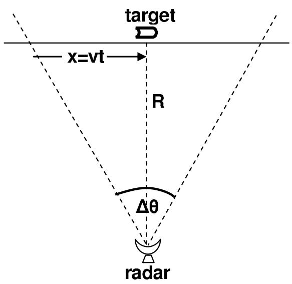

Figure 1. A target moving perpendicularly past a monochromatic CW radar.

For this geometry, Brown (1967) defines the point target response of a monochromatic CW radar as

$$W(x) = A\left(\frac{x}{r}\right)\exp\left(j\frac{4\pi}{\lambda}\sqrt{r^2 + x^2}\right). \tag{3}$$

Computation of the instantaneous frequency of the response allows the bandwidth to be written as

$$B = \frac{4\pi}{\lambda}\frac{x}{\sqrt{r^2 + x^2}} = \frac{4\pi}{\lambda}\sin\left(\frac{\Delta\theta}{2}\right) \tag{4}$$

and hence the cross range resolution is given by

$$\Delta x = \frac{\pi}{B} = \frac{\lambda}{4\sin(\Delta\theta/2)}. \tag{5}$$

For a linear, stripmap-mode synthetic aperture, equation (5) reduces to $\Delta x = d/2$, which is independent of both range and frequency. Even higher resolution can be obtained with a spotlight-mode synthetic aperture, steering the real-aperture beam (either mechanically or electronically) to keep the target scene in view for a longer period, and hence forming a longer synthetic aperture. Thus as $\Delta\theta \to 180°$, the cross range resolution $\Delta x \to \lambda/4$.

A practical maximum value for $\Delta\theta$ is likely to be no more than 60°, leading to $\Delta x \approx \lambda/2$, for real systems limited by practical considerations such as range ambiguity, range curvature, SNR, etc.

The equivalent result for range resolution may be obtained by writing (1) as

$$\Delta r = \frac{c}{2B} = \frac{\lambda}{2}\frac{f_0}{B}. \tag{6}$$

The fractional bandwidth, B/f_0 could in principle be 200%, with the signal bandwidth extending from zero to $2f_0$, and giving $\Delta r = \lambda/4$, but a practical maximum value is likely to be closer to 100%, giving $\Delta r \approx \lambda/2$.

In the last year or so results have appeared in the open literature which approach this limit (Brenner and Ender, 2004), (Cantalloube and Dubois-Fernandez, 2004). Figure 2 shows one example from a recent conference of an urban target scene. Critical to the ability to produce such imagery is the ability to characterise and compensate for platform motion errors, since in general the platform will not move with perfectly uniform motion in a straight line. Of course, motion compensation becomes most critical at the highest resolutions. This is conventionally achieved by a combination of inertial navigation (IN) and autofocus processing, and a number of different autofocus algorithms have been devised and evaluated (Oliver and Quegan, 1998). In practice IN sensors are sensitive to rapidly-varying errors and autofocus techniques are best able to correct errors which vary on the same spatial scale as the synthetic aperture length, so the two techniques are essentially complementary.

It is possible to improve the resolution in images using so-called superresolution image processing techniques. Under most favourable conditions an improvement of a factor of between 2 and 3 in image resolution is achievable, though to achieve this it is necessary that the signal-to-noise ratio should be adequately high (at least 20 dB) to start with and that imagery should be free from artefacts.

Other means of extracting information from the target scene, and hence of providing information to help discriminate the target from clutter and to classify the target, include (i) interferometric processing to provide high-resolution three-dimensional information on target shape; (ii) polarimetric radar, since the polarimetric scattering properties of targets and of clutter may be significantly different, especially if the target includes dihedral or trihedral-like features; and (iii) multi-aspect imaging, since views from different aspects of a target will almost certainly provide greater information to assist the classification process (Baker et al., 2006).

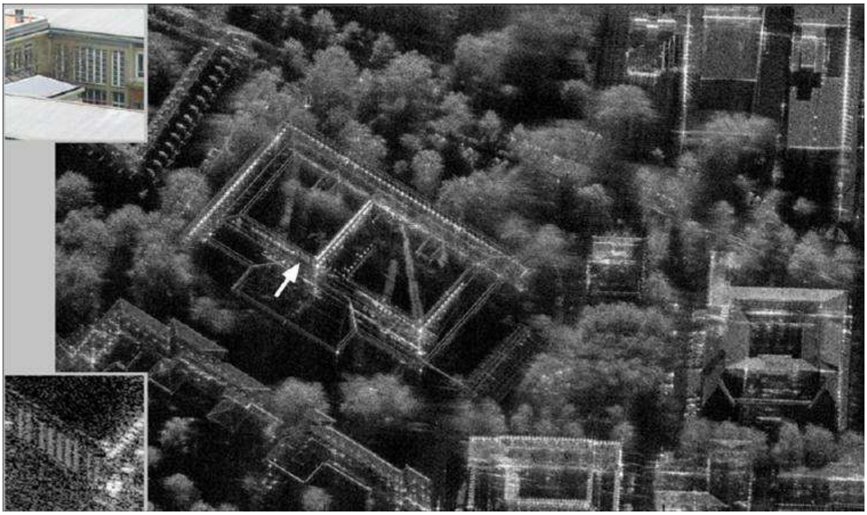

Figure 2. High resolution aircraft-borne SAR image of a part of the university campus in Karlsruhe (Germany). The white arrow refers to a lattice in the left courtyard, which is shown in more detail in the small picture on the left bottom. The corresponding optical image is shown on the left top (after Brenner and Ender (2004)).

3. Applications to counterterrorism

3.1. RADAR DETECTION OF BURIED TARGETS

An important application is the use of radar to detect and classify objects buried in the ground. Specifically in a counterterrorism context such objects may take the form of landmines and Improvised Explosive Devices (IEDs), weapons caches, and tunnels, though other applications include archaeology and the detection of buried pipes and cables. Fundamental to such applications are the propagation characteristics of electromagnetic radiation through soil, and at the boundary between air and soil, and how these characteristics depend on frequency and on soil properties. In general it can be appreciated that a lower frequency may give lower propagation loss than a higher frequency, but will in general give poorer resolution, both in range and in azimuth.

Daniels (2004) has provided a comprehensive account of the issues in Ground Penetrating Radar (GPR) and examples of systems and results. He states that '... GPR relies for its operational effectiveness on successfully meeting the following requirements:

(a) efficient coupling of electromagnetic radiation into the ground;

(b) adequate penetration of the radiation through the ground having regard to target depth;

(c) obtaining from buried objects or other dielectric discontinuities a sufficiently large scattered signal for detection at or above the ground surface;

(d) an adequate bandwidth in the detected signal having regard to the desired resolution and noise levels.'

Daniels provides a table of losses for different types of material at 100 MHz and 1 GHz (Table I) and presents a taxonomy of system design options (Figure 3). The majority of systems use an impulse-type waveform and a sampling receiver, processing the received signal in the time domain. More recently, however, FMCW and stepped frequency modulation schemes have been developed, which require lower peak transmit powers. Both types of systems, though, require components (particularly antennas) with high fractional bandwidths, which are not necessarily straightforward to realise.

TABLE I. Material loss at 100 MHz and 1 GHz (after Daniels (2004) © IET, 2004).

Material	Loss at 100 MHz	Loss at 1 GHz
Clay (moist)	5–300 dB m^{-1}	50–3000 dB m^{-1}
Loamy soil (moist)	1–60 dB m^{-1}	10–600 dB m^{-1}
Sand (dry)	0.01–2 dB m^{-1}	0.1–20 dB m^{-1}
Ice	0.1–5 dB m^{-1}	1–50 dB m^{-1}
Fresh water	0.1 dB m^{-1}	1 dB m^{-1}
Sea water	100 dB m^{-1}	1000 dB m^{-1}
Concrete (dry)	0.5–2.5 dB m^{-1}	5–25 dB m^{-1}
Brick	0.3–2 dB m^{-1}	3–20dB m^{-1}

As an example of the results that can be achieved, Figure 5 shows images of a buried antipersonnel mine at a depth of 15 cm, showing both the original image and the results after image processing techniques have been used to enhance the target.

3.2. THROUGH-WALL RADAR IMAGING

The ability to image targets through building walls, to detect and classify personnel and objects within rooms, is of significant importance in counterterrorism operations, and there has been a great deal of work on the subject in the last

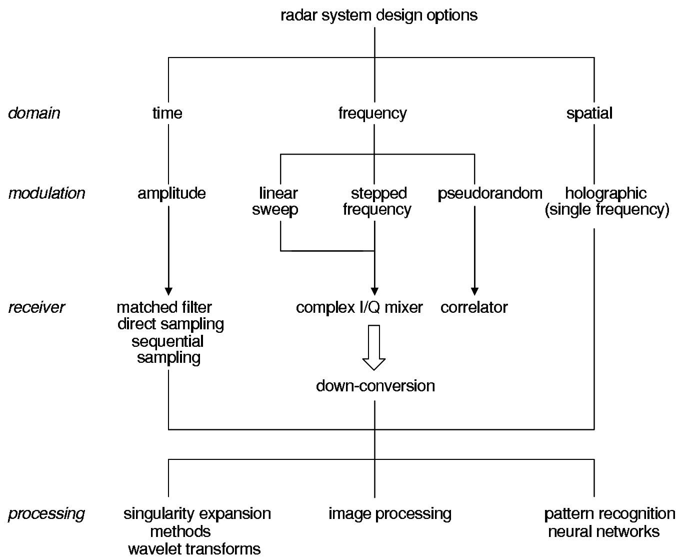

Figure 3. System design and processing options for Ground Penetrating Radar (after Daniels (2004) © IET, 2004).

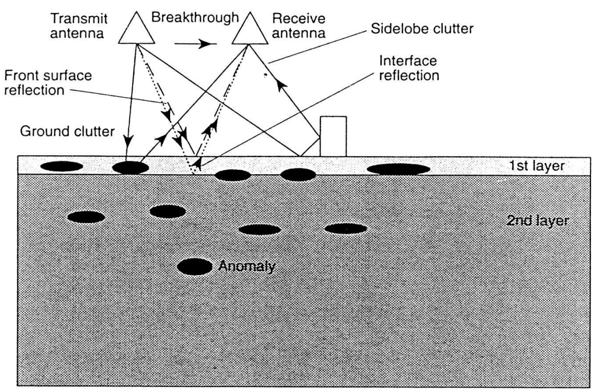

Figure 4. Physical layout of Ground Penetrating Radar system (after Daniels (2004) © IET, 2004).

decade. Essentially similar considerations to those for Ground Penetrating Radar apply, in that a lower frequency may give lower propagation loss than a higher frequency, but will in general give poorer resolution, both in range and in azimuth. The final line of Table I shows the attenuation of brick at frequencies of 100 MHz and 1 GHz, but many internal building walls may be made of material of lower attenuation.

Police officers, search and rescue workers, urban-warfare specialists and counterterrorism agents may often encounter situations where they need to detect, identify, locate and monitor building occupants remotely. An ultra high resolution

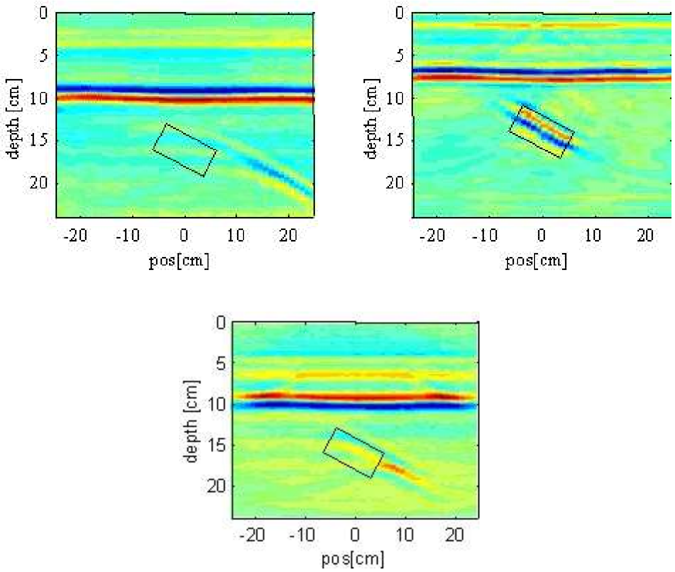

Figure 5. Oblique antipersonnel mine at an angle of 30°: (a) B-scan of raw data; (b) after migration by deconvolution; (c) after Kirchhoff migration (after Daniels (2004) © IET, 2004).

through-wall imaging radar has the potential for supplying this key intelligence in a manner not possible with other forms of sensor. High resolution and the ability to detect fine Doppler such as heart beat movements enable a detailed picture of activity to be built up so that appropriate and informed decisions can be made as to how to tackle an incident. For example, in a hostage scenario the layout of a room can be established and it may be possible to differentiate hostage from terrorist. An escaping suspect hidden behind a bush or wall can be detected and tracked. Alternatively, in the aftermath of a terrorist event, people buried in rubble but alive can be detected on the basis of radar reflections from their chest cavity, thus helping to direct rescue workers to best effect.

Key enabling technology and techniques are:

- Distributed aperture sensing for very high ($\sim\lambda$ or better) cross-range resolution in both azimuth and elevation dimensions;
- Ultra wideband pulsed waveforms (to give wavelength equivalent range resolution);
- Novel near-field focus tomographic processing;
- Narrow band adjunct waveforms for fine Doppler discrimination.

Whilst aspects of each of these has been reported individually (Aryanfar and Sarabandi (2004), Song et al. (2005), Yang and Fathy (2005)), there has been little or no research combining them to generate wavelength-sized resolution in three dimensions enabling fine discrimination of internal objects (e.g. an individual holding a gun could be potentially identified and position determined against background furniture). Much of the technology necessary already exists and can be procured at low cost (of the order of a few thousand pounds, aided by the fact that transmitter powers need only be a fraction of a Watt). The key research challenges lie primarily in developing processing techniques and algorithms that allow a wavelength (< 10 cm) resolution whilst avoiding unacceptable sidelobes and ambiguities and to do this over extended spatial areas. In addition the approach also includes use of a Doppler waveform with very high resolution. To achieve all this requires a combination of distributed aperture near-field processing coupled with reflection based tomography. Lastly, information extraction from the resulting imagery remains a major challenge in radar; however, this should be considerably aided by the very high resolutions to be employed. There is a great deal of interest in this area as evidenced by the DARPA Visibuilding program. This is investigating a wide variety of sensor and processing techniques with the aim of providing a comprehensive internal picture within urban and sub-urban environments (`http://www.darpa.mil/baa/baa06-04.html`). At the heart of any solution is likely to be through wall technology of the type indicated above.

3.3. TOMOGRAPHY AND DETECTION OF CONCEALED WEAPONS

The techniques of tomography have been developed originally for medical imaging, to provide 2D cross-sectional images of a 3D object from a set of narrow X-ray views of an object over the full 360° of direction. The results of the received signals measured from various angles are then integrated to form the image, by means of the Projection Slice Theorem. The Radon Transform is an equation derived from this theorem which is used by various techniques to generate tomographic images. Two examples of these techniques are Filtered Backprojection (FBP) and Time Domain Correlation (TDC). Further descriptions of these techniques may be found in Soumekh (1999).

In radar tomography the observation of an object from a single radar location can be mapped into Fourier space. Coherently integrating the mappings from multiple viewing angles enables a three dimensional projection in Fourier space. This enables a three dimensional image of an object to be constructed using conventional tomography techniques such as wavefront reconstruction theory and backprojection where the imaging parameters are determined by the occupancy in Fourier space. Complications can arise when target surfaces are hidden or masked at any stage in the detection process. This shows that intervisibility characteristics of the target scattering function are partly responsible for determining the imaging properties of moving target tomography. In other words, if a scatterer on an object is masked it cannot contribute to the imaging process and thus no resolution improvement is gained. However, if a higher number of viewing angles are employed then this can be minimised. Further complications may arise if (a) the point scatterer assumption used is unrealistic (as in the case of large scatterers introducing translational motion effects), (b) the small angle imaging assumption does not apply and (c) targets with unknown motions (such as non-uniform rotational motions) create cross-product terms that cannot be resolved.

The Tomographic Reconstruction (TR) algorithm applies the Projection-Slice theorem of the Fourier transform to compute the image. The Projection-Slice theorem states that the 1D Fourier transform of the projection of a 2D function, $g(x, y)$ made at an angle w is equal to a slice of the 2D Fourier transform of the function at an angle w (see Figure 6).

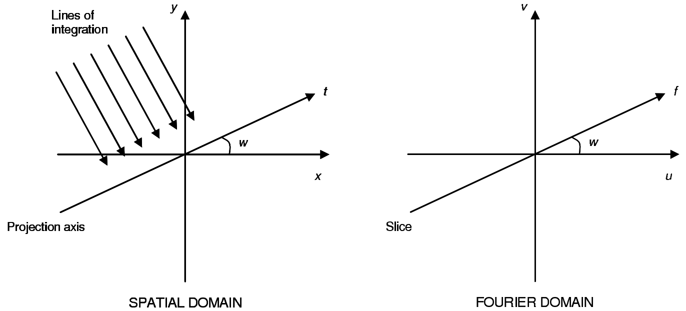

Figure 6. Tomographic reconstruction: the Projection Slice Theorem.

Whereas some algorithms convert the outputs from many radars simultaneously into a reflectivity image using a 2D Fourier transform, TR generates an image by projecting the 1D Fourier transform of each radar projection individually back onto a 2D grid of image pixels. This operation gives rise to the term Backprojection. The image can be reconstructed from the projections using the Radon transform. The equation below shows this

$$g(x, y) = \int_0^\infty \int_{-\infty}^\infty P(f) \cdot |f| \cdot e^{j2\pi f (x\cos(w) + y\sin(w))} df\, dw \qquad (7)$$

where

w = projection angle
$P(f)$ = the Fourier transform of the 1-D projection $p(t)$.

The Filtered Backprojection (FBP) method may be used to process by reconstructing the original image from its projections in two steps: Filtering and Backprojection.

Filtering the projection: The first step of FB Preconstruction is to perform the frequency integration (the inner integration) of the above equation. This entails filtering each of the projections using a filter with frequency response of magnitude $|f|$.

The filtering operation may be implemented by ascertaining the filter impulse response required, then performing convolution or a FFT/IFFT combination to correlate $p(t)$ against the impulse response.

Backprojection: The second step of FB Preconstruction is to perform the angle integration (the outer integration) of the above equation. This projects the 1D filtered projection $p(t)$ onto the 2D image by following these steps: Next place a pixel-by-pixel rectangular grid over the XY plane. Then place the 1D filtered projection $p(t)$ in position at angle w. For each pixel: Get position of the sample needed from the projection angle and pixel position. Interpolate the filtered projection to obtain the sample. Add this backprojection value multiplied by the angle spacing. Repeat the whole process for each successive projection.

Tomography of Moving Targets

A development of these concepts has been the idea of imaging of moving targets using measurements from a series of multistatic CW or quasi-CW transmissions, giving rise to the term ‘ultra narrow band’ (UNB) radar. This may be attractive in situations of spectral congestion, in which the bandwidth necessary to achieve high resolution by conventional means (equation (1)) may not be available. Narrow band CW radar is also attractive as peak powers are reduced to a minimum, sidelobes are easier to control, noise is reduced and transmitters are generally low cost. Applications may range from surveillance of a wide region to the detection of aircraft targets, to the detection of concealed weapons carried by moving persons. In general the target trajectory projection back to a given radar location will determine resolution. A random trajectory of constant velocity will typically generate differing resolutions in the three separate dimensions. However, even if there is no resolution improvement there will be an integration gain due to the time series of radar observations. A Hamming window or similar may be required to reduce any cross-range sidelobe distortions. The treatment which follows is taken from that of Bonneau, Bascom, Clancy and Wicks (2002).

Figure 7 shows the relationship between the bistatic sensor geometry and the representation in Fourier space. The bistatic angle is B and the bistatic bisector is the vector $\mathbf{u_B}$.

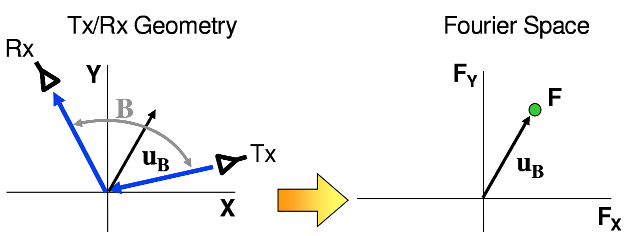

Figure 7. Relationship between bistatic sensor geometry and representation in Fourier space (after Bonneau et al. (2002)).

The corresponding vector **F** in Fourier space is given by

$$\mathbf{F} = \frac{4\pi f}{c} \cos\left(\frac{B}{2}\right) \cdot \mathbf{u_B}. \tag{8}$$

Figure 8 shows the equivalent relationship for a monostatic geometry. The resolutions are inversely proportional to the sampled extents Δu and Δv in Fourier space, thus

$$\Delta r = \frac{2\pi}{\Delta u} \qquad \Delta r = \frac{2\pi}{\Delta v} \tag{9}$$

which should be compared to equations (1), (2) and (5).

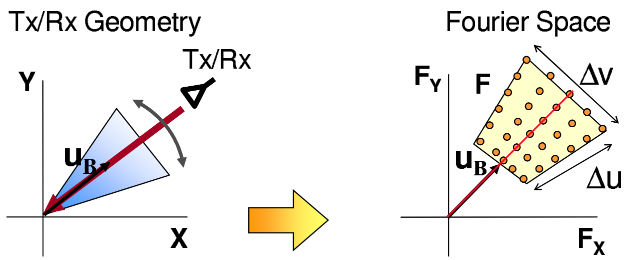

Figure 8. Fourier space sampling and scene resolution for a monostatic SAR (after Bonneau et al. (2002)).

In an UNB radar the finite bandwidth of the radar signal limits the range resolution. However, this resolution can be recovered by multistatic measurements over a range of angles. Figure 9 shows four examples, and the Fourier space sampling corresponding to each.

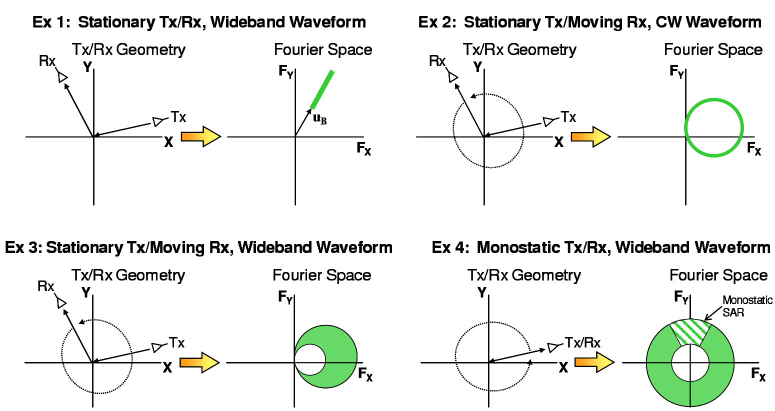

Figure 9. Fourier space sampling and scene resolution for four examples: (i) stationary tx/rx, wideband waveform; (ii) stationary tx, moving rx, CW waveform; (iii) stationary tx, moving rx, wideband waveform; (iv) monostatic tx/rx, wideband waveform (after Bonneau et al. (2002)).

Recent experimental work under controlled conditions in anechoic chambers (Wicks et al. (2005), Wicks (2005)) and using turntable-mounted targets (Coetzee et al., 2006) has demonstrated the validity of these theoretical approaches, and may be expected to pave the way for more practical experiments and systems.

3.4. PASSIVE mm-WAVE IMAGING

Although not strictly a radar technique, one form of imaging that has shown significant counterterrorism applications is passive mm-wave imaging. Here, an image is formed at mm-wave frequencies (typically 35 or 94 GHz) of the thermal energy radiated or reflected from a target scene, in a similar way to thermal infrared imaging. However, the angular resolution (equation (2)) of an aperture of a given size is significantly poorer at mm-wave frequencies, so to achieve equivalent image resolution a significantly larger sensor aperture is necessary. On the other hand, in contrast to thermal infrared imaging, the transmission properties of radiation at these frequencies are such that mm-wave signals are not significantly attenuated by obscurants such as smoke or fog, or in particular by clothing.

The image contrast is due to the difference between emissive sources which appear warm (~290 K) and reflective (metallic) objects which reflect cold sky (~80 K at W-band) and hence which appear cold.

Figure 10. (left) MITRE passive mm-wave imager; (right upper) optical image from Malvern Hills; (right lower) equivalent passive mm-wave image (courtesy of QinetiQ).

Figure 10 shows an example of an image obtained by a system of this kind, from the Malvern Hills in the west of the UK, on a summer day. Whilst the optical image is rather hazy, the mm-wave image is much clearer. The physical aperture of the imager is 1.2 m, giving an angular resolution at 94 GHz of ~2.5 mrad, and the image is formed by mechanical scanning of the antenna, taking several seconds to build up the image. The receiver technology uses broad bandwidth low-noise amplifiers ahead of a detector; these achieve noise figures of a few dB and several tens of dB of gain, but the millimetre-wave MMICs requires specialised fabrication facilities.

More formally, we can write down an equation which relates the temperature sensitivity ΔT of a radiometer to the system noise temperature T_{sys}, the RF bandwidth B and the integration time τ:

$$\Delta T = \frac{T_{sys}}{\sqrt{B\tau}}. \tag{10}$$

The number of resolution cells (i.e. pixels) N is the product of the image width X and image height Y, divided by the resolution cell size δ^2:

$$N = \frac{XY}{\delta^2}. \tag{11}$$

If the number of simultaneous beams (receivers) is n, then the image acquisition time T is given by:

$$T = \frac{N}{n}\tau \tag{12}$$

and so

$$T = \frac{N}{n} \cdot \frac{1}{B}\left(\frac{T_{sys}}{\Delta T}\right)^2. \tag{13}$$

This demonstrates the tradeoffs involved in a passive mm-wave imaging system, and shows that if high-resolution images are to be obtained at operationally-useful frame rates ($T \ll 1$ second), multiple receiver channels will be necessary. Several types of scanning have been evaluated: mechanical, electronic, optical and digital. Some elegant forms of mechanical scanning have been devised (Appleby et al., 1997).

Figure 11. (left) passive mm-wave image of a person with a concealed weapon; (right) corresponding optical image (courtesy of QinetiQ, Malvern).

In the context of counterterrorism the technique has shown great promise in detection of concealed weapons. Figure 11 shows an image of a person with a concealed gun, and the corresponding optical image. When used indoors, some form of low-level noise illumination is needed. Figure 12 shows the result of fusing an optical image (which would show the identity of the individual) with a passive mm-wave image.

Figure 12. Image fusion and detection (image courtesy Farran Technology 94GHz scanning system and ERA Technology).

3.5. PASSIVE BISTATIC RADAR

Although not strictly an imaging radar technique, there is considerable current interest in passive bistatic radar (PBR), making use of 'illuminators of opportunity' such as broadcast, communications or radionavigation signals, rather than dedicated radar transmissions. Such illuminators - particularly VHF FM radio and UHF television - are high power and have very wide coverage, although digital radio and television signals are more favourable in certain respects. Passive bistatic radar systems have several attractive features: (i) the radar system is passive, and hence undetectable (at least, by means of any radiated signal); (ii) reduced complexity and cost, since the transmit hardware already exists; (iii) it allows the use of frequency bands (VHF and UHF) which are not normally available for radar use; and (iv) the bistatic geometry offers a counterstealth capability against certain types of target.

One type of threat for which passive bistatic radar systems may be particularly well suited is the defence of high-value assets such as government buildings, power stations or defence establishments against small airborne vehicles, such as low-flying light aircraft, gliders or unmanned air vehicles (AUVs), which might carry explosive, chemical or biological warheads. Examples of incidents involving such threats in recent years include the landing of a light aircraft in Red Square, Moscow, in 1987, the attack on the Pirellone Building in Milan, Italy, in May 2002, and the landing of a light aircraft close to the White House in Washington DC in May 2005 (Figure 13). Small air platforms of this kind will have much lower radar cross section than conventional aircraft, so although conventional surveillance radar systems may in principle give coverage of these areas, their ability to detect such low-signature targets may be somewhat limited. The

Figure 13. Three examples of incidents involving low-signature aircraft threats : (i) light aircraft landing in Red Square, Moscow in 1987; (ii) Pirellone Building, Milan, 18 April 2002; (iii) White House, Washington DC, 12 May 2005.

properties of illumination sources for passive bistatic radar, and the detection performance against different targets, have been evaluated and discussed (Baker et al. (2005), Griffiths and Baker (2005a), Griffiths and Baker (2005b)). Detection and tracking of conventional commercial aircraft (whose RCS would be of the order of 20 dBm^2) at ranges in excess of 100 km, using VHF FM radio transmissions, have been demonstrated, and these results can be extrapolated to predict the performance against low signature targets of the type shown in Figure 13. Such systems would therefore be usable as ‘gap fillers’ for regions where the coverage of conventional surveillance sensors is inadequate, or to protect particular high-value assets. Another application might be against low-signature maritime targets, such as might be used to attack high-value naval targets, or for gun- or drug-running, although it is necessary to be sure that the illuminator coverage out to sea is adequate (Willis and Griffiths, 2007).

4. Future prospects

We have shown that there is a great deal of valuable information that can be gleaned by using radar sensors. It is equally clear that alone they do not provide a trouble free route to reliable imaging, resulting in the detection of terrorist threats. Indeed as terrorists become more sophisticated they may well use jamming and deception techniques, a topic that we have not even considered here. Nevertheless, the promise shown by these radar based approaches, both individually and collectively, certainly makes it worth investing in their further development. Specifically, low cost high resolution is key where fine detail is required, such as for the identification of concealed weapons. Wide area sensors based on low cost, passive concepts and able to fill gaps left, for example, by current Air Defences need to be fully understood if optimum performance is to be achieved. The areas of maximising dynamic range and coping with transmitted waveforms of an unknown type will be drivers for immediate research. Overall it is clear that there are many differing challenges for a wide variety of sensor systems. However, the benefit in greatly improved capability provides more than sufficient motivation for overcoming them.

Acknowledgements

We gratefully acknowledge the assistance of Professor Mike Wicks and his colleagues (AFRL), Dr. Roger Appleby (QinetiQ) and David Daniels (ERA Technology) in the preparation of this paper, both for the provision of results and figures and for invaluable discussions. We also thank the organisations, including the UK Ministry of Defence, the US Air Force Office of Scientific Research, the UK Engineering and Physical Sciences Research Council, QinetiQ and its predecessors, BAE SYSTEMS, Thales Sensors and AMS, who have supported the various pieces of work whose results are reported here.

References

Appleby, R., Gleed, D., and Lettington, A. H. (1997) The military applications of passive millimetre-wave imaging, *Journal of Defence Science* **2**.

Aryanfar, F. and Sarabandi, K. (2004) Through wall imaging at microwave frequencies using space-time focusing, In *IEEE Intl. Antennas and Propagation Symposium*, Vol. 3, pp. 3063–3066.

Ausherman, D. A., Kozma, A., Walker, J. L., Jones, H. M., and Poggio, E. C. (1984) Developments in radar imaging, *IEEE Trans. Aerospace & Electronics Systems* **AES–20**, 363–400.

Baker, C. J., Griffiths, H. D., and Papoutsis, I. (2005) Passive Coherent Radar systems - part II: waveform properties, In IEE (ed.), *Special Issue of IEE Proc. Radar, Sonar and Navigation on Passive Radar Systems*, Vol. 152, pp. 160–168.

Baker, C. J., Vespe, M., and Griffiths, H. D. (2006) *Multi-perspective imaging and image interpretation*, Il Ciocco, Italy.

Bell, M. (1993) Information theory and radar waveform design, *IEEE Trans. Information Theory* **39**, 1578–1597.

Bonneau, R. J., Bascom, H. F., Clancy, J. T., and Wicks, M. C. (2002) Tomography of moving targets (TMT), Italy.

Brenner, A. R. and Ender, J. H. G. (2004) Airborne SAR imaging with subdecimetre resolution, In *Proc. EUSAR 2004 Conference*, pp. 267–270, Ulm.

Brown, W. M. (1967) Synthetic aperture radar, *IEEE Trans. Aerospace & Electronic Systems* **AE 3–3**, 217–229.

Cantalloube, H. and Dubois-Fernandez, P. (2004) Airborne X-band SAR imaging with 10 cm resolution - technical challenge and preliminary results, In *Proc. EUSAR 2004 Conference*, pp. 271–274, Ulm.

Carrara, W., Goodman, R. S., and Majewski, R. M. (1995) *Spotlight Synthetic Aperture Radar: Signal Processing Algorithms*, Artech House.

Coetzee, S., Baker, C. J., and Griffiths, H. D. (2006) Narrow band high resolution radar imaging, In *Proc. IEEE Radar Conference 2006*, pp. 622–625, Verona, 24–27 April 2006.

Daniels, D. J. (2004) *Ground Penetrating Radar (2nd edition)*, ISBN 0-86341-360-9, Peter Peregrinus, Stevenage.

Griffiths, H. D. and Baker, C. J. (2005)a 'Fundamentals of tomography and radar' 'Bistatic and multistatic sensors for homeland security', In *NATO Advanced Study Institute Advances in Sensing with Security Applications, Il Ciocco, Italy*, ISBN 1-4020-4286-8.

Griffiths, H. D. and Baker, C. J. (2005)b Passive Coherent Radar systems - part I: performance prediction, In IEE (ed.), *Special Issue of IEE Proc. Radar, Sonar and Navigation on Passive Radar Systems*, Vol. 152, pp. 153–159.

Howland, P. E., Maksimiuk, D., and Reitsma, G. (2005) FM radio based bistatic radar, In IEE (ed.), *Special Issue of IEE Proc. Radar, Sonar and Navigation on Passive Radar Systems*, pp. 107–115, June 2005.

Knaell, K. K. and Cardillo, G. P. (1995) Radar tomography for the generation of three-dimensional images, *IEE Proc. Radar, Sonar and Navigation on Passive Radar Systems* **142**, 54–60.

Munson, D. C. J., O'Brien, J. D., and Jenkins, W. K. (1983) A tomographic formulation of spotlight-mode synthetic aperture radar, In *Proc. IEEE*, Vol. 71, pp. 917–925.

Oliver, C. J. and Quegan, S. (1998) *Understanding SAR Images*, Artech House.

Pasmurov, A. Y. and Zinoviev, Y. (2005) *Radar Imaging and Tomography*, Peter Peregrinus, Stevenage.

Sakamoto, T. and Sato, T. (1999) A target shape estimation algorithm for pulsed radar systems based on boundary scattering transform, In *IEICE Trans. Commun.*, Vol. E78–B.

Soldovieri, F., Brancaccio, A., Leonore, G., and Pieri, R. (2005) Shape reconstruction of perfectly conducting objects by multi view eperimental data, *IEEE Trans. Geoscience & Remote Sensing* **43**, 65–71.

Song, L.-P., Yu, C., and Liu, Q. H. (2005) Through-wall imaging (TWI) by radar: 2-D tomographic results and analyses, *IEEE Trans. Geoscience and Remote Sensing* **43**, 2793–2798, December 2005.

Soumekh, M. (1999) *Synthetic Aperture Radar Signal Processing with MatLab Algorithms*, Artech House.

`http://www.darpa.mil/baa/baa06-04.html`.

Vespe, M., Baker, C. J., and Griffiths, H. D. (2005) Multi-perspective target classification, In *Proc. RADAR 2005 Conference*, pp. 877–882, IEEE Publ. No. 05CH37628, Washington DC, 9-12 May 2005.

Walker, J. L. (1980) Range Doppler imaging of rotating objects, *IEEE Trans. Aerospace & Electronics Systems* **16**, 23–52.

Wehner, D. R. (1987) *High Resolution Radar*, Artech House.

Wicks, M. (2005) Tomography, Waveform Diversity and Intelligent Systems, In *AOC Fourth Multinational Conference on Passive and Covert Radar*, Syracuse, 5-7 October 2005.

Wicks, M. C., Himed, B., Bascom, H., and Clancy, J. (2005) Tomography of Moving Targets (TMT) for security and surveillance, In *NATO Advanced Study Institute Advances in Sensing with Security Applications, Il Ciocco, Italy*, ISBN 1-4020-4286-8.

Wiley, C. A. (1985) Synthetic Aperture Radars - a paradigm for technology evolution, *IEEE Trans. Aerospace & Electronic Systems* **AES–21**, 440–443.

Willis, N. and Griffiths, H. D. (2007) *(eds), Advances in Bistatic Radar*, to be published by SciTech, 2007.

Yang, Y. and Fathy, A. E. (2005) See-through-wall imaging using ultra wideband short-pulse radar system, In *IEEE Intl. Antennas and Propagation Symposium*, Vol. 3B, pp. 334–337, 3–8 July 2005.